

## Direct Measurement of Vanadium Crossover in an Operating Vanadium Redox Flow Battery

David C. Sing, Jeremy P. Meyers  
Materials Science and Engineering,  
The University of Texas, Austin, Texas 78712, USA

Measurements of Vanadium diffusion coefficients for transport across cation exchange membranes using dialysis cells have been reported in the literature. However, to date direct measurement of crossover coefficients in an operating Vanadium redox flow battery (VRB) cell have not been reported. Results are reported in this paper on experiments utilizing a special VRB cell which allows measurement of Vanadium ion transport across ion exchange membranes with and without the presence of current. The cell utilizes two additional flow regions which collect Vanadium ions which diffuse from the positive and negative half cells. The effects of the magnitude and direction of electrical current on transport can be measured directly with this cell. We observe that transport is greatly enhanced when the direction of the hydrogen ion flux is in the same direction as the density gradient driven vanadium flux and suppressed when the hydrogen ion flux is in the opposite direction. The cell has been used to investigate the effects on transport of current densities up to  $900 \text{ mA/cm}^2$ .

### Introduction

The all Vanadium Redox flow Battery (VRB) has been proposed as an ideal system for grid level energy storage. The decoupling of storage capacity from power capacity that is characteristic of all flow batteries combined with the use of Vanadium ions for both the positive and negative electrolyte components make the VRB an attractive candidate for high capacity low maintenance energy storage systems. An essential component of the VRB is the ion exchange membrane. The ion exchange membrane has two competing roles: maintaining separation of the electrolyte species while providing a high conductivity path for hydrogen ions to complete the electrical circuit within the VRB. It is usually thought that a thinner membrane is desirable for its lower voltage drop compared to a thicker membrane of the same type, but this advantage is compromised by higher cross-over rates which can degrade the long term capacity of the VRB. However, the results reported in this work suggest that thicker membranes may not have an advantage in terms of reduced cross-over at current densities in excess of  $450 \text{ mA/cm}^2$ .

### Brief Review of Previous Ion Cross-over Measurements

#### Dialysis Cell Results

Several groups have reported measurements of Vanadium cross-over using dialysis cells [1,2,3]. In these experiments vanadium ion solutions are circulated through a cell in which an ion exchange membrane has been mounted. On the other side of the membrane a solution of sulfuric acid is circulated with an equivalent sulfate concentration as the vanadium solution to minimize osmotic pressure effects. Due to the concentration gradient

Vanadium ions diffuse through the ion exchange membrane and the concentration of Vanadium can be measured using UV/VIS spectroscopy [1,2] or by potentiometric titration [3]. Mass transport coefficients and diffusion coefficients for  $V^{+2}$ ,  $V^{+3}$ ,  $V^{+4}$ , and  $V^{+5}$  can be found using this method. However, in an operating VRB, an electrical current primarily carried by the  $H^+$  ions is also present, and with it an electro-osmotic flow of water. Vanadium ions can also be transported by convective flow as well as by electro-migration. These effects cannot be measured in dialysis cell experiments. Note that in this paper the tetravalent Vanadium ion is written as  $V^{+4}$  although it exists as in the form of a  $VO^{+2}$  ion, similarly Vanadium in the +5 ionization state is written as  $V^{+5}$  but actually exists as a  $VO_2^+$  ion.

### VRB Cell Results

Luo and co-workers [4] measured vanadium ion transport in a redox flow battery using a mixed Vanadium/Fe system. In these experiments Vanadium redox couples ( $V^{+2}/V^{+3}$  or  $V^{+4}/V^{+5}$ ) were paired with the  $Fe^{+2}/Fe^{+3}$  redox couple to form a working flow battery cell. Vanadium which crossed over to the Fe side of the cell was measured using ICP mass spectroscopy (ICP/MS). In these experiments, the total concentration of Vanadium crossing over can be measured but that of the individual ionic components cannot be determined. The authors isolated the effects of state of charge chemical composition changes from electrically driven transport changes by combining four different cells in a series/parallel arrangement. The effects of current densities up to  $50 \text{ mA/cm}^2$  were investigated in these experiments. The authors found that transport was enhanced when the electrical current was in the same direction as the ion gradient driven flux and suppressed with the electric current was in the opposite direction.

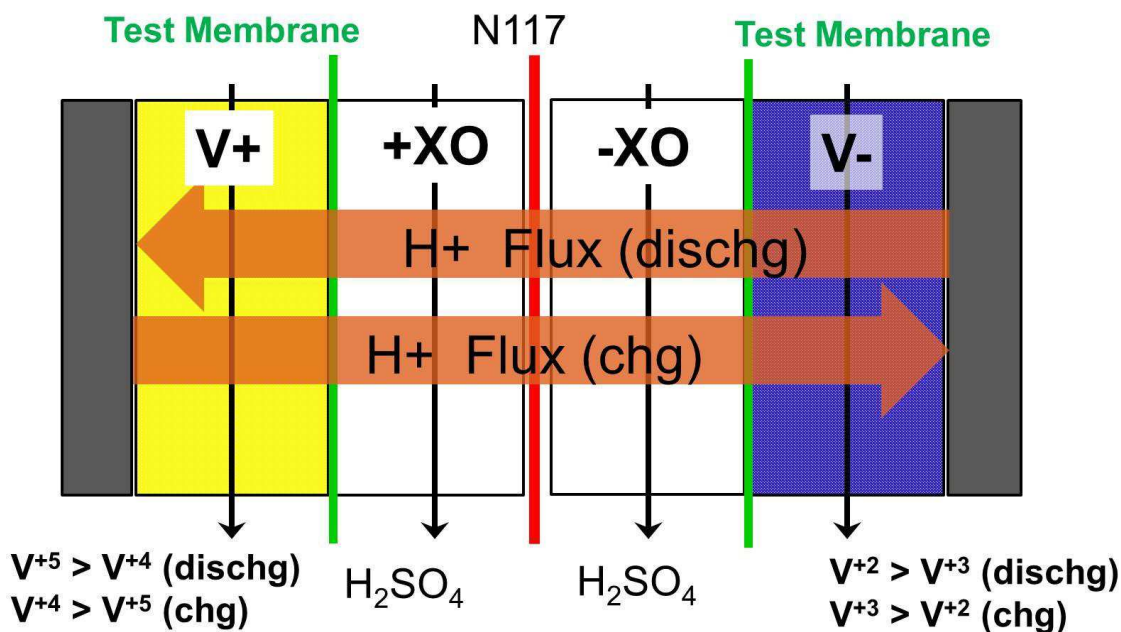


Figure 1. Triple Membrane Cross-Over (XO) Cell for studying ionic cross-over through ion exchange membranes.

### Triple Membrane VRB Cell for Ion Cross-over Measurements

A novel VRB cell has been developed by our group which allows the measurement of Vanadium cross-over with and without the presence of electrical current in a single cell. Figure 1 shows schematic view of the new cell. The new cell adds two additional flow regions between the usual V+ and V- half cells of a VRB. The new regions are referred to as the “Cross-over” (XO) regions, abbreviated +XO and -XO for the cross-over regions adjacent to the V+ and V- half cells respectively. The XO regions are separated from the V+ and V- regions with ion exchange membranes, and a third ion exchange membrane separates the two XO regions from each other. The usual V<sup>+4</sup>/V<sup>+5</sup> electrolyte solution circulates through the V+ region and a V<sup>+2</sup>/V<sup>+3</sup> electrolyte mixture circulates through the V- region. An H<sub>2</sub>SO<sub>4</sub> solution circulates through the XO regions of the cell with a separate flow circuit for +XO and -XO regions. This special triple membrane cell is referred to as the “XO cell” since it contains the dedicated subsections to collect cross-over ions. The XO cell facilitates direct measurement of Vanadium species which are transported across the ion exchange membranes which separate the XO regions from their neighboring half cells. Because the concentration of Vanadium in the half cells is much greater than the concentration in either of the XO regions, the transport of V into the XO regions is dominated by transport from the neighboring half cells and cross-talk between the two XO cells should be negligible. The experimental results show this to be the case.

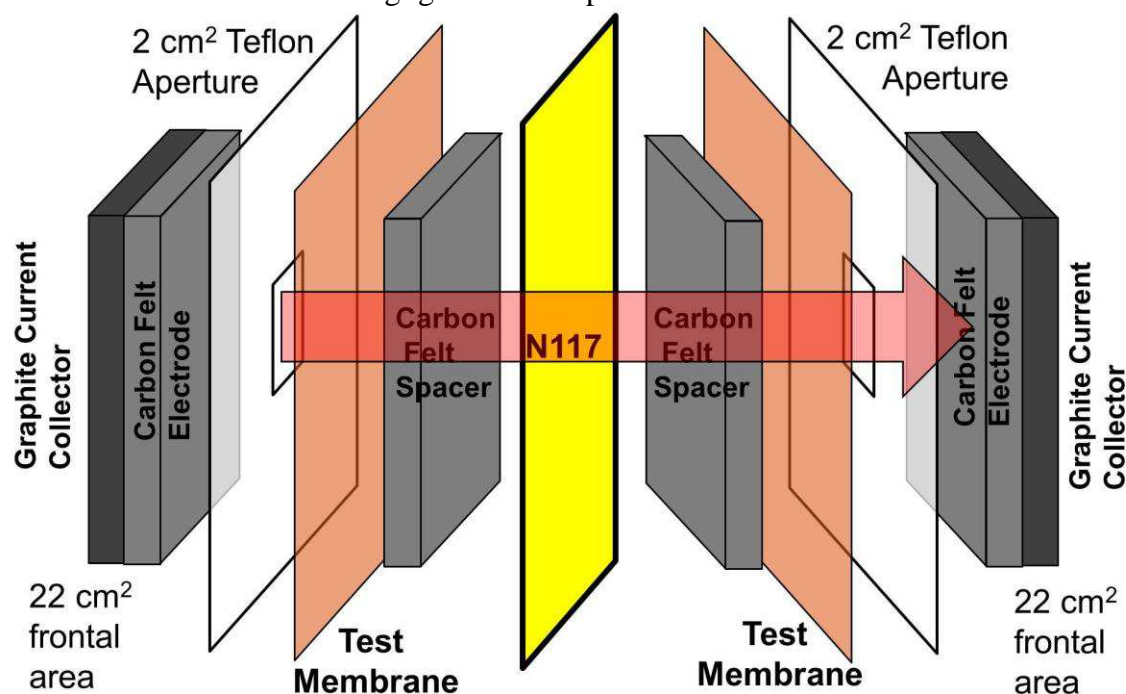


Figure 2. Exploded view of XO Cell

Figure 2 shows an exploded view of the XO cell. The outer regions of the cell, V+ and V-, are conventional in design, with graphite current collectors and graphite felt porous electrodes which fill the gap between the membranes and the current collectors. The XO regions of the cell are separated from the half cells by the ion exchange membranes to be tested. In these experiments, three different kinds of membranes were tested: Nafion<sup>TM</sup> N212 and N117, and Fumatech<sup>TM</sup> VX7050. In the XO regions, porous electrodes are included to maintain the spacing between the test membranes and a center membrane made of N117. The porous electrodes in the XO regions are not in direct contact with any

external electrodes. Sandwiched between the test membranes and the V<sup>+</sup> or V<sup>-</sup> porous electrodes is a thin Teflon™ sheet (75 μm) with a 2 cm<sup>2</sup> aperture which concentrates the current through passing through the test membranes. Current densities of up to 900 mA/cm<sup>2</sup> have been run in the experiments reported in this paper.

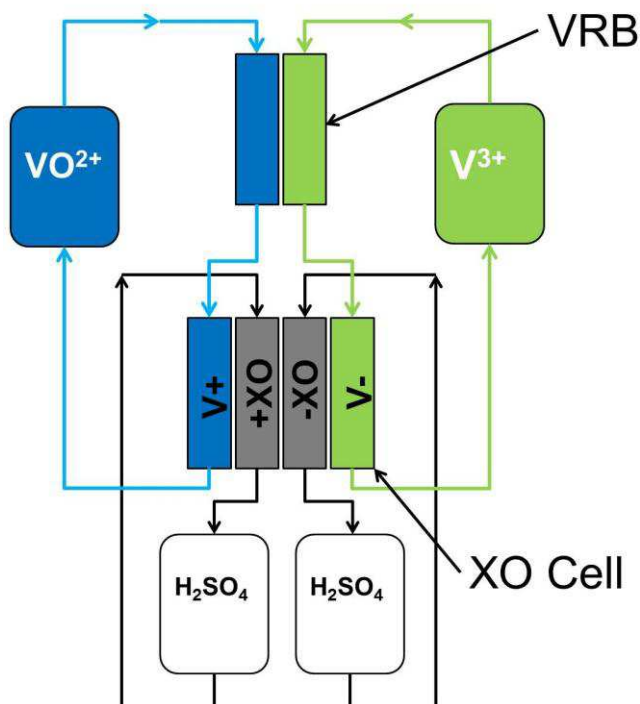


Figure 3. Experimental Arrangement for XO Cell Experiments

Figure 3 shows the experimental layout for these experiments. The V<sup>+</sup> and V<sup>-</sup> electrolytes are circulated through the V<sup>+</sup> and V<sup>-</sup> half cells using a peristaltic pump. Glass reservoirs and acid resistant plastic tubing are used throughout. The XO regions each have their own flow circuit with a separate reservoir and peristaltic pump channel. All the reservoirs are flooded with an inert Argon atmosphere to prevent unintended oxidation of the Vanadium ions. A conventional VRB shares the XO cell V<sup>+</sup> and V<sup>-</sup> flow circuit. The XO cell can be run as a conventional VRB in which case the second VRB cell is used to measure the open circuit voltage (OCV) which gives an indication of the state of charge (SOC) of the vanadium electrolyte solutions. Alternatively, the second VRB can be used to run a charge or discharge cycle while the XO cell is run with zero current. In this manner the effect of current flow on Vanadium transport can easily be isolated from that of V<sup>+</sup>/V<sup>-</sup> electrolyte composition changes due to SOC changes.

### UV/VIS Absorption Spectroscopy Measurements

Throughout this work UV/VIS spectroscopy is used to determine the concentrations of the electrolytes in the V<sup>+</sup> and V<sup>-</sup> regions as well as in the solutions circulating through the XO regions. At the beginning and end of each experiment run a 1 ml sample of electrolyte is removed from the V<sup>+</sup> and V<sup>-</sup> reservoirs. The sample is diluted (10:1 for total V concentrations < 1M, 20:1 for total V concentrations > 1M) before an absorption spectrum is measured from 360 to 900 nm using a Milton-Roy Spectronic 3000 spectrometer. The composition and concentration of V<sup>+2</sup>/V<sup>+3</sup> and V<sup>+4</sup>/V<sup>+5</sup> mixtures can be

found by comparing the mixture spectrum against the spectrums of known reference concentrations of  $V^{+2}$ ,  $V^{+3}$ ,  $V^{+4}$ , and  $V^{+5}$ . In all cases the spectrums of  $V^{+2}/V^{+3}$  and  $V^{+4}/V^{+5}$  samples can be fit with a linear combination of the reference spectrums. There have been no issues with fitting mixtures of  $V^{+4}/V^{+5}$  to reference spectrums when the  $V^{+}$  samples have been diluted sufficiently. The +XO and -XO samples are sufficiently dilute that no additional dilution is needed to be able fit the sample spectrums and determine the ionic composition.

### XO Cell Cross-over Experiments

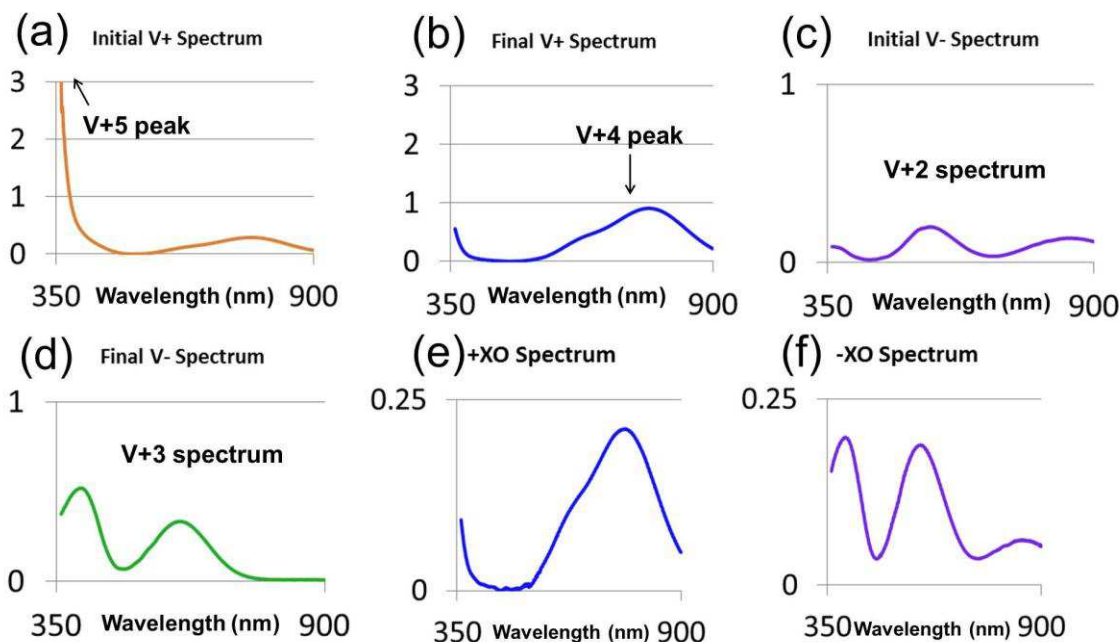


Figure 4. Absorption spectra for XO cell running a 600 mA discharge. (a) Initial V+ (b) Final V+ (c) Initial V- (d) Final V- (e) +XO Spectrum (f) -XO Spectrum

### Full Cell Mode Experiments

Figure 4 shows the absorption spectra data for the XO cell running in a discharge cycle with a current of 600 mA. The current through the cell was controlled using an Arbin battery testing system for all the experiments reported in this paper. The cell was initially charged with 180 ml V+ electrolyte with a mixture of  $V^{+4}/V^{+5}$  at 75% SOC. The V- reservoir contained 125 ml of nearly 100%  $V^{+2}$ . After a 10800 second 600 mA discharge the V+ reservoir was at a 15% SOC and the solution in the V- reservoir was nearly completely converted to  $V^{+3}$ . Hence the initial spectrum of the V+ electrolyte shown in Figure 4(a) has a very strong absorption at the blue end of the spectrum, characteristic of  $V^{+5}$ , while the spectrum in Figure 4(b) shows a strong peak at 760 nm characteristic of  $V^{+4}$ . Similarly, the V- spectrum shown in Figure 4(c) is initially that of  $V^{+2}$  and at the end of the discharge is that of  $V^{+3}$  as shown in Figure 4(d). The XO reservoirs of the cell were initially charged with 30 ml of 4M  $H_2SO_4$  solution. During the discharge the +XO and -XO regions accumulated Vanadium which crossed over from the V+ and V- regions. At the end of the experiment the XO samples were analyzed in the spectrometer. Figure 4(e) shows the spectrum of the +XO solution and Figure 4(f) shows



the spectrum of the  $-XO$  solution. It can be seen from the figures that the spectrum of the  $+XO$  sample is a linear combination of the  $V^{+4}$  and  $V^{+5}$  spectra while the  $-XO$  samples has contributions only from  $V^{+2}$  and  $V^{+3}$ .

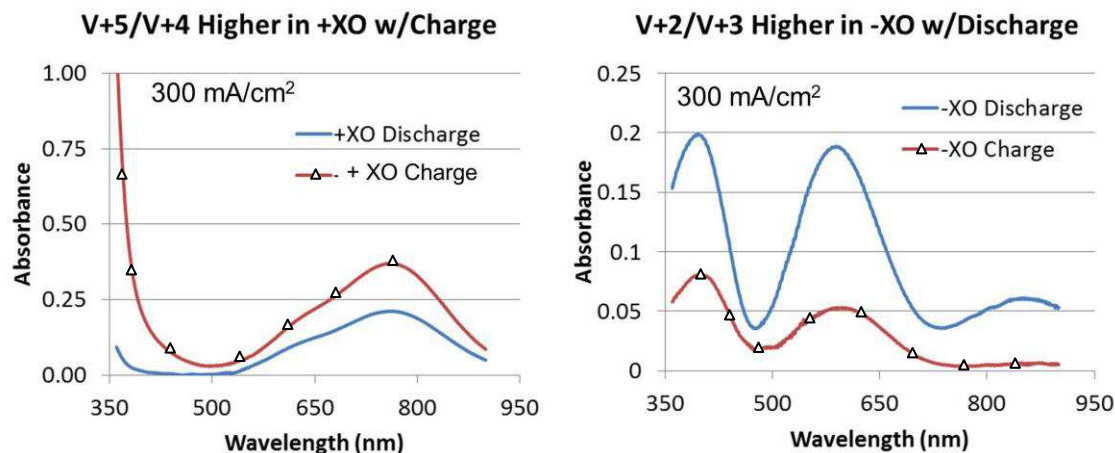


Figure 5. Comparison of  $+XO$  and  $-XO$  spectra with Charge and Discharge

At the end of the discharge experiment the XO regions of the XO cell are purged with deionized water to remove any traces of Vanadium and the XO reservoirs are reloaded with fresh charges of 30 ml  $H_2SO_4$  solution. The cell was then run in the charge mode with the same magnitude of current and time duration. At the end of the experiment the  $V+$  and  $V-$  electrolytes were restored to nearly their original state and the fresh  $+XO$  and  $-XO$  samples were collected for analysis. Figure 5 compares the spectrums for the  $+XO$  and  $-XO$  solutions for the charge and discharge experiments. It can be seen from Figure 5 that the absorption, and hence Vanadium concentration, in the  $+XO$  region is much higher during charge than discharge, while the reverse is true in the  $-XO$  region. During the charge mode, the  $H+$  flux is in the  $V+$  to  $V-$  direction, so both the  $H+$  flux and the electric field are parallel with the direction of concentration gradient driven flux of  $V^{+4}/V^{+5}$  into the  $+XO$  region and opposite to the direction of the concentration gradient driven flux of  $V^{+2}/V^{+3}$  from the  $V-$  region into the  $-XO$  region. The changes in Vanadium transport with current direction are in agreement the results reported in [4] from the mixed  $V/Fe$  flow battery experiments.

### Half Cell Mode Experiments

Although the XO cell is capable of running the full cell reaction with both the  $V^{+2}/V^{+3}$  and  $V^{+4}/V^{+5}$  redox couples, most of the experiments were run in the half cell mode, in which both the  $V+$  and  $V-$  sides of the cell are running the same redox reaction, with one side running the reaction in the oxidation direction and the other side running the reaction in the reduction direction. Figure 6 shows the absorption data spectra for the XO cell running a 1200 mA charge cycle with the  $V+$  electrolyte initially consisting of nearly 100%  $V^{+4}$  and the  $V-$  electrolyte with nearly 100%  $V^{+5}$ . The Arbin battery tester was used to drive the oxidation reaction  $V^{+4}$  to  $V^{+5}$  on the  $V+$  side and the reduction reaction  $V^{+5}$  to  $V^{+4}$  on the  $V-$  side. The  $H+$  flux is from the  $V+$  side to the  $V-$  side. After one hour the  $V+$  electrolyte was nearly 100% converted to  $V^{+5}$  and the reverse was true of the  $V-$  electrolyte. The XO samples both show absorption spectra which are linear

combinations of  $V^{+4}$  and  $V^{+5}$  spectra but the +XO absorption is significantly higher than the -XO absorption. This result is consistent with the result seen with the full cell reaction, in which the Vanadium transport is enhanced when the  $H^+$  flux is in the direction of the concentration gradient flux and suppressed with the  $H^+$  flux opposes the concentration gradient flux.

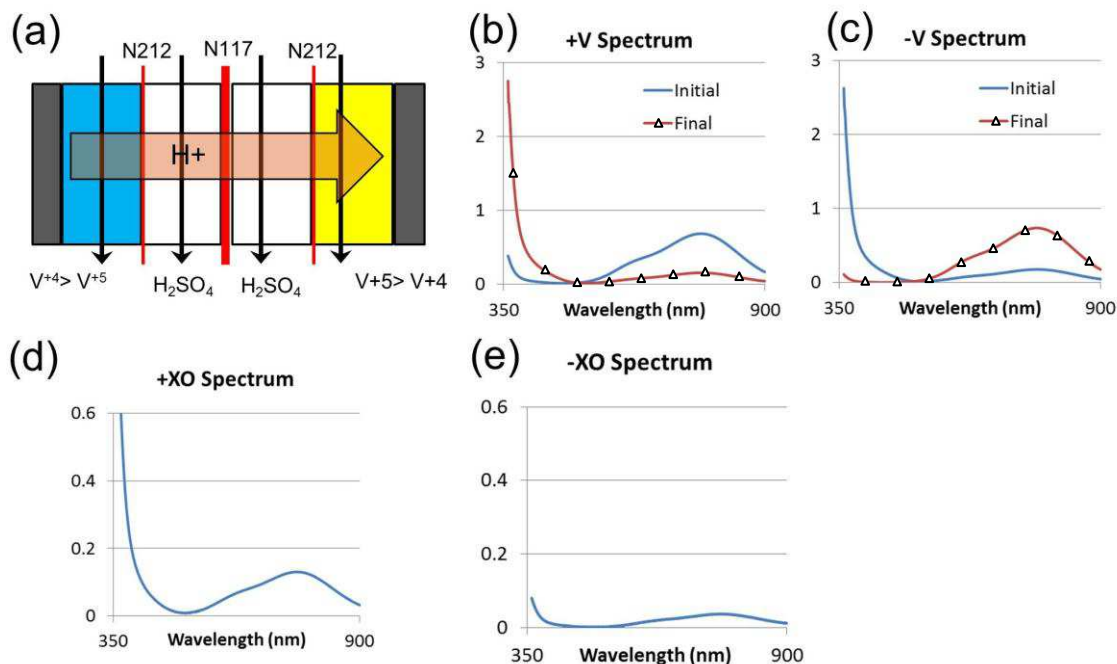


Figure 6. (a) Experimental arrangement for  $V^{+4}/V^{+5}$  half cell mode experiments (b)  $V^{+4}$  absorption spectra (c)  $V^{+5}$  spectra (d) +XO spectrum (e) -XO spectrum.

### Data Analysis

The absorption spectra as shown in Figures 4, 5, and 6 are used to compute mass transport coefficients for Vanadium. For transport of ionic species  $i$  through the membrane separating the +XO and  $V^{+4}$  regions of the XO cell, the mass transfer coefficient  $m$  is calculated from the initial concentration of  $i$  in the  $V^{+4}$  region,  $C_{i,V^{+4}}(t_i)$ , the final concentration,  $C_{i,V^{+4}}(t_f)$ , and the final concentration in the +XO region  $C_{i,+XO}$  as:

$$m = \frac{\text{Vol} * C_{i,+XO}}{T * (C_{i,V^{+4}}(t_i) + C_{i,V^{+4}}(t_f)) / 2} \quad (1)$$

where Vol is the volume of the fluid in the XO reservoir and T is the experiment time. Implicit in this formula is the assumption that the concentration varies linearly with time (good for constant current reactions) and that the mass transport coefficient does not depend on concentration. The mass transport coefficient as defined above is useful for comparing the results of many experiments in which the experiment time, current densities, and initial and final concentrations may vary. Hidden within in this definition are the transport effects which are not concentration gradient driven, for example migration due to electric field or transport due to convective flows. Electric field and

convective flow effects will lead to larger or smaller transport coefficients compared to the zero field and zero flow values.

### Variation of $V^{+4}/V^{+5}$ Cross-over with Current Density

A series of experiments were performed using the  $V^{+4}/V^{+5}$  redox couple with the XO cell running in the half cell mode. Total Vanadium concentration in the test solutions was 0.7M in 3M sulfuric acid. Deionized water was pumped through the XO regions of the cell to flush out any residual Vanadium from the system before a fresh charge of 30 ml of 4M  $H_2SO_4$  was loaded to the XO reservoirs prior to the start of each experiment. Currents between 600 mA and 1800 mA were run through the cell. Samples of the  $V^{+4}$  and  $V^{+5}$  electrolytes were taken and diluted to determine the initial and final electrolyte compositions using UV/VIS absorption spectroscopy and the XO electrolytes were measured without dilution to measure the amount of Vanadium which crossed through the N212 test membranes.

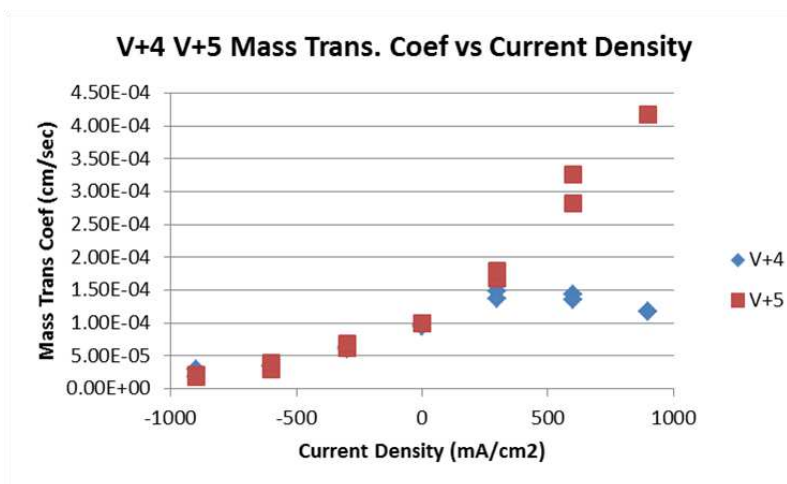


Figure 7.  $V^{+4}/V^{+5}$  Mass transport coefficients vs. Current density through N212 membranes.

Figure 7 shows the measured  $V^{+4}$  and  $V^{+5}$  mass transport coefficients as a function of current density through N212 membranes. Positive current density corresponds to  $H^+$  flux flowing into the XO cell from the adjacent half cell, while negative current density corresponds to  $H^+$  flux flow out of the XO cell to the adjacent half cell. Figure 7 shows that the both the  $V^{+4}$  and  $V^{+5}$  mass transport coefficients are enhanced by positive current densities, but surprisingly the  $V^{+4}$  mass transport begins to saturate at a current density of +300  $mA/cm^2$  while the  $V^{+5}$  mass transport coefficient continues to increase. The  $V^{+4}$  and  $V^{+5}$  mass transport coefficients decrease significantly as the current density becomes more negative, with both reduced to less than 25% of the zero current value.

Three different ion exchange membranes were compared in a second series of experiments: N212, N117, and VX7050. The electrolyte solutions used for these experiments were prepared from 1.5M  $VOSO_4$  and 3.5M  $H_2SO_4$ , and 5M  $H_2SO_4$  was circulated through the +XO and -XO regions of the XO cell to collect Vanadium which is transported through the test membranes. Figure 8 shows the  $V^{+4}$  and  $V^{+5}$  mass transport



coefficients plotted against current density for these three membranes. The two Nafion membranes have similar behavior at high positive current densities, at zero current and negative current densities the thicker N117 exhibits less transport. Transport through the VX7050 membrane was less than either of the Nafion membranes for all the conditions tested, but the voltage required to drive the equivalent current was always significantly higher (>50%) than for the Nafion membranes. As was seen with the earlier experiments with N212 using 0.7M Vanadium solutions, the transport coefficient for the  $V^{+5}$  species diverges from that of  $V^{+4}$  for high positive current densities.

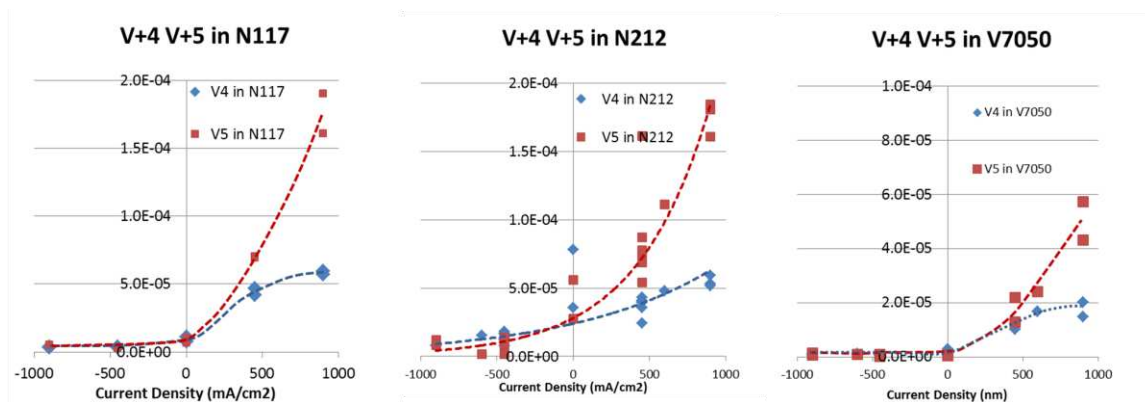


Figure 8.  $V^{+4}/V^{+5}$  Mass transport coefficient vs. Current density for N117, N212, and Fumatech VX7050 membranes.

Figure 9 shows the total Vanadium mass transfer coefficient as a function of current densities for all three membrane types on the same graph. The combined mass transfer coefficient for transport from the  $V^{+}$  to the  $+XO$  region is calculated from the measured Vanadium concentrations using:

$$m = \frac{\text{Vol} * (C_{V^{+4},+XO} + C_{V^{+5},+XO})}{T * \langle C_{V,V^{+}} \rangle} \quad (2)$$

In the above expression  $\langle C_{V,V^{+}} \rangle$  is the average Vanadium concentration in the  $V^{+}$  region of the cell and is calculated using :

$$\langle C_{V,V^{+}} \rangle = C_{V^{+4},V^{+}} + C_{V^{+5},V^{+}} \quad (3)$$

Since the average Vanadium concentration is nearly constant this quantity can be evaluated with either the initial or final  $VO^{+2}$  and  $VO_2$  samples from the  $V^{+}$  half cell. The equivalent expression is used for the transport from  $V^{-}$  to  $-XO$  regions. Figure 9 shows that the difference in transport between N212 and N117 disappears for current densities greater than  $450 \text{ mA/cm}^2$ , but for lower current densities transport through N212 is always greater than that through N117.

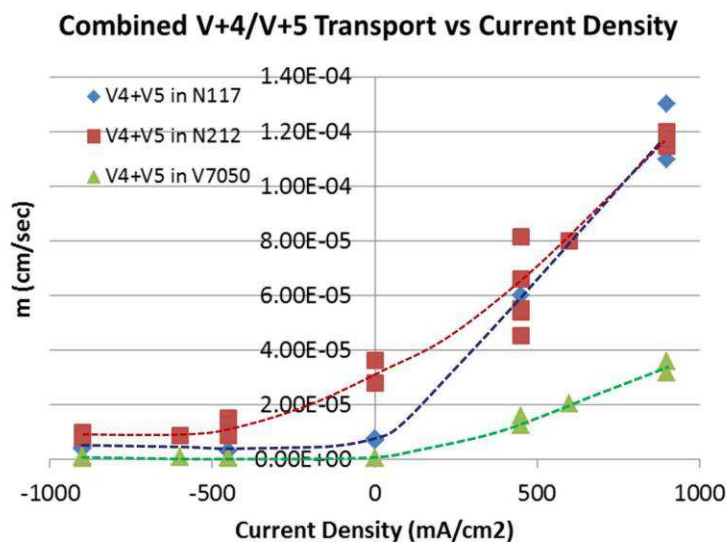


Figure 9. Combined  $V^{+4}/V^{+5}$  Mass transport coefficient vs. Current density for N117, N212, and VX7050 membranes.

### $V^{+3}/V^{+4}$ Cross-over Experiments

A third series of experiments was conducted to investigate the transport of  $V^{+4}$  using the  $V^{+3}/V^{+4}$  redox couple in the XO cell running in the half cell mode. Comparison of mass transfer coefficients calculated from  $V^{+3}/V^{+4}$  and  $V^{+4}/V^{+5}$  experiments provides insight into the origin of the apparent saturation of the  $V^{+4}$  transport coefficient as current density increases as observed in the  $V^{+4}/V^{+5}$  experiments.

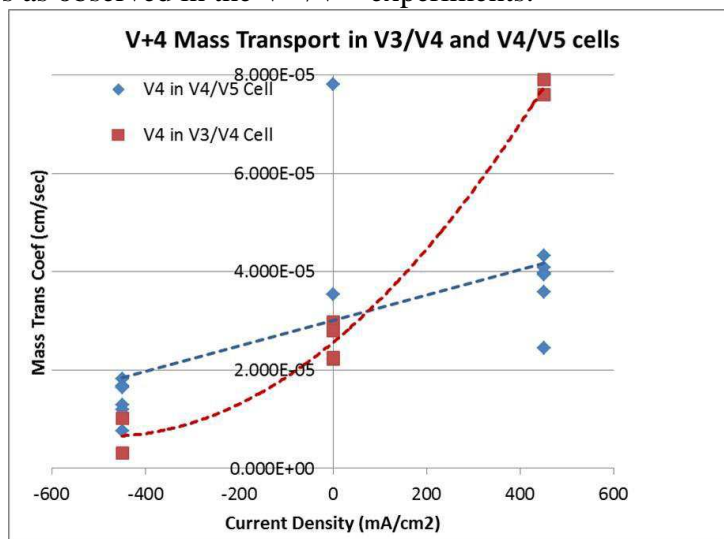


Figure 10.  $V^{+4}$  Mass transport coefficient vs. Current density for  $V^{+3}/V^{+4}$  and  $V^{+4}/V^{+5}$  experiments.

Figure 10 compares the  $V^{+4}$  mass transfer coefficients from the  $V^{+3}/V^{+4}$  experiments against the equivalent data from the  $V^{+4}/V^{+5}$  experiments. The mass transfer coefficient at 450 mA/cm<sup>2</sup> current for  $V^{+4}$  is much larger for the  $V^{+3}/V^{+4}$  reaction compared to the  $V^{+4}/V^{+5}$  reaction.  $V^{+4}$  is the product of the reaction  $V^{+3} \rightarrow V^{+4} + e^{-1}$  while it is the reactant in the reaction  $V^{+4} \rightarrow V^{+5} + e^{-1}$ . This suggests a mechanism to explain the

divergence in the  $V^{+4}$  and  $V^{+5}$  mass transfer coefficients at positive current densities which was observed in all the experiments using the  $V^{+4}/V^{+5}$  reaction. If the reaction  $V^{+4} \rightarrow V^{+5} + e^{-1}$  was occurring the +XO region of the XO cell during the  $V^{+4}/V^{+5}$  experiments  $V^{+4}$  is converted to  $V^{+5}$  and the apparent mass transfer rate of  $V^{+5}$  is enhanced while that of  $V^{+4}$  is suppressed, In the  $V^{+3}/V^{+4}$  experiments a similar mechanism would convert  $V^{+3}$  to  $V^{+4}$  leading to an enhancement in the apparent mass transfer rate of  $V^{+4}$  at the expense of  $V^{+3}$ . However, for the oxidation reaction (either  $V^{+4} \rightarrow V^{+5} + e^{-1}$  or  $V^{+3} \rightarrow V^{+4} + e^{-1}$ ) to occur in the XO region a pathway for the electron generated in the reaction to reach the current collector attached to the V+ half cell must exist as illustrated in Figure 11.

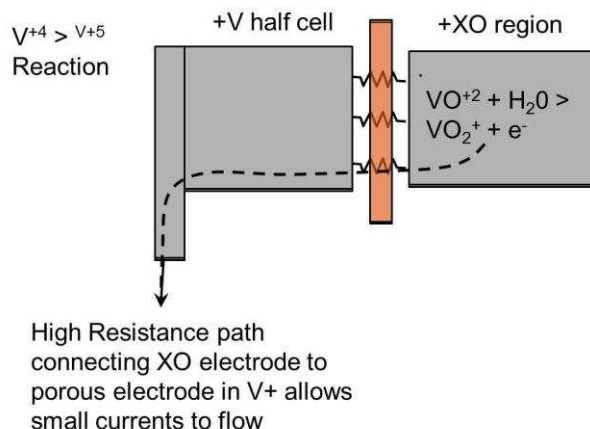


Figure 11. High resistance path connecting +XO porous electrode to the V+ electrode provides a pathway to allow oxidation reaction of  $V^{+4}$  to  $V^{+5}$  to occur within the +XO region of the XO cell.

### Summary and Conclusions

A novel triple membrane redox flow battery cell optimized to measure cross-over of electrolyte species across ion exchange membranes has been designed and tested. The cell, referred to as the “cross-over” (XO) cell, can be used with any redox system, although it was tested in these experiments using the all Vanadium system. Strong enhancement in  $V^{+4}$  and  $V^{+5}$  ion transport is observed with the  $H^{+}$  flux is in the direction of the concentration driven flux and greatly suppressed when the current flow is reversed. At current densities greater than  $300 \text{ mA/cm}^2$  the measured mass transport coefficient of  $V^{+4}$  begins to saturate while that of  $V^{+5}$  increase greatly. This behavior is observed with N212, N117, and Fumatech VX7050 cation exchange membranes. It is proposed that the divergence in the mass transfer coefficients is due to oxidation of the  $V^{+4}$  to  $V^{+5}$  after it has diffused through the ion exchange membrane.

### Acknowledgments

This work is supported by the US Department of Energy ARPA-E program grant # DE-AR00000149

## References

1. F. Grossmith, P. Llewellyn, A.G. Fane, M. Skyllas-Kazacos, "Evaluation of membranes for all-vanadium redox cell", Proc. Electrochem. Soc. Symp., Honolulu, October 1988, pp. 363-374.
2. E. Wiedemann, A. Heintz, R.N. Lichtenthaler, J. Membrane Science, **141**, 215-221 (1998).
3. C. Sim, J. Chen, H. Zhang, X. Han, Q. Luo, J. Power Sources, **195**, 890-897 (2010).
4. Q. Luo, L. Li, Z. Nie, W. Wang, X. Wei, B. Li, B. Chen, Z. Yang, J. Power Sources, **218**, 15-20, (2012).